

RSC Advances



This is an *Accepted Manuscript*, which has been through the Royal Society of Chemistry peer review process and has been accepted for publication.

Accepted Manuscripts are published online shortly after acceptance, before technical editing, formatting and proof reading. Using this free service, authors can make their results available to the community, in citable form, before we publish the edited article. This *Accepted Manuscript* will be replaced by the edited, formatted and paginated article as soon as this is available.

You can find more information about *Accepted Manuscripts* in the [Information for Authors](#).

Please note that technical editing may introduce minor changes to the text and/or graphics, which may alter content. The journal's standard [Terms & Conditions](#) and the [Ethical guidelines](#) still apply. In no event shall the Royal Society of Chemistry be held responsible for any errors or omissions in this *Accepted Manuscript* or any consequences arising from the use of any information it contains.



Journal Name

ARTICLE

Tumor cell responses to carbon dots derived from chondroitin sulfate

Shujun Wang,^{‡ a,b} Beibei Wang,^{‡ b,c} Fengwu Bai,^{a*} and Xiaojun Ma^{b**}

Received 00th January 20xx,
Accepted 00th January 20xx

DOI: 10.1039/x0xx00000x

www.rsc.org/

Mass production of carbon-dots (CDs) derived from chondroitin sulfate (CS) were developed by the facile hydrothermal approach for the first time. The CS derived CDs (CSCDs) possessed good dispersibility and water solubility, bright blue and green luminescence, and relatively pH- and photostable property. Moreover, the multicolor CSCDs could be efficiently uptaken by SAS cells and exhibited low cytotoxicity. Therefore, the responses of human oral squamous cell carcinoma SAS cells to CSCDs were further investigated by evaluating their proliferation and invasion. Compared to CS, CSCDs not only provided higher efficiency for proliferation of SAS cells, and up-regulated expression of matrix metalloproteinases to mimic extracellular matrix secretion, but also portrayed fluorescence for labeling SAS tumor cells. Hence, the multifunctional CSCDs were expected to have potential for biomedical applications.

Introduction

Carbon-dots (CDs) have been the subject of intensive research due to their unique properties such as good water-solubility, low cytotoxicity, eco-friendliness, biocompatibility and particularly their easily tuned optical properties and resistance to photodegradation,¹⁻⁶ which have been applied in various areas including environmental monitoring, disease diagnostics, bio-imaging and proteomic and genomic studies.⁷⁻⁹ Organic substances such as proteins, amino acids, saccharides and small molecules like citrate acid etc have been explored as carbonaceous sources for producing CDs.¹⁰ However, natural materials are always preferred for this purpose. For instance, CDs have been synthesized from alginate, a negatively charged polysaccharide.¹¹

As a natural glycosaminoglycan with good biocompatibility, chondroitin sulfate (CS) is a potential candidate for manufacturing CDs with low cytotoxicity. CS is an anionic linear chain attached onto specific scaffolds, forming a major extracellular matrix (ECM) on the cell surface.¹² Despite simplicity of the backbone structure, the CS polymer is complex enough to mediate the cell-cell and cell-ECM interactions that are essential for carrying biological information, and thus determine many biological functions.^{13,14} For example, CS could strongly influence the proliferation, even migration of malignant tumor cells.^{15,16} With high anionic activity, CS can

interact with various ligands and receptors, and in turn activate signaling pathways,^{13,17-19} stimulating the growth, migration and metastasis of tumor cells. Previous studies reported that treating tumors with chondroitinase AC led to the reducing growth and invasion of tumor cells.²⁰ Meanwhile, free exogenous CS also exerted effects on the FGF-2-induced proliferative response in melanoma cells.²¹ CS is the receptor of CD44, which is overexpressed in metastatic cancer tissue, and has been used as anionic components of ternary complexes in drug delivery systems for cancer treatment.²²⁻²⁴ CS polymer has been demonstrated to play an important role in creating microenvironment for protease activation by binding matrix metalloproteinase2 (MMP2) through the C-domain.²⁵ MMP2 is one of the family members of MMPs, which, as zinc-dependent proteolytic enzymes, are capable of degrading various components of ECM and bioactive molecules,²⁶ and thus are associated with tumor progression, even invasion and metastasis.^{27,28} Chemically synthesized CS hexasaccharides also enhanced the CD44 cleavage and promoted tumor cell motility in a CD44-dependent manner.²⁴ Thus, the CS derived CDs (CSCDs) are expected to remain the functionality of CS, which is vital for tissue engineering research. Moreover, nanotechnology has made it possible to design and fabricate biomimetic microenvironment at nanoscale, providing nanoparticles to emulate native ECM.²⁹ Meanwhile, living cells are highly sensitive to local nanoscale topographic patterns within ECM,^{30,31} so building nanostructures is a promising approach to mimic native cellular microenvironments.

Herein, a straightforward route using CS as carbonaceous source was developed for manufacturing luminescent CDs with the CS characters of influencing tumor cell proliferation and invasion, which would provide a powerful bio-imaging agent with good biocompatibility to examine the specific mechanisms of tumor cell proliferation and invasion.

^aSchool of Life Science and Biotechnology, Dalian University of Technology, Dalian 116023, China. Fax: +86-411-84706308, fwbai@dlut.edu.cn.

^bDivision of Biotechnology, Dalian Institute of Chemical Physics, Chinese Academy of Sciences, 457 Zhongshan Road, Dalian 116023, China; Fax: +86-411-84379139, maxj@dicp.ac.cn.

^cUniversity of the Chinese Academy of Sciences, Beijing 100049, China.

[‡]Shujun Wang and Beibei Wang contributed equally to this work.

Experimental

Materials and cell line

CS and Gelatin were purchased from Sigma-Aldrich (St. Louis, MO, USA). Quinine sulfate was purchased from Aladdin. Sodium chloride (>99.5%) and sodium hydroxide (>96%) was purchased from Dalu Chemical Reagent Co. Ltd (Tianjin, China). Phosphate (H_3PO_4 >85%) was purchased from Hengxing Chemical Reagent Co. Ltd. (Tianjin, China). Boric acid (H_3BO_3 >99.5%) was purchased from Bodi Chemical Reagent Co. Ltd. (Tianjin, China). Ammonium persulfate, tetramethylethylenediamine (TEMED) and Tris base were purchased from Solarbio (Beijing, China). Acrylamide, glycine and N, N'-methylene-bis-(acrylamide) were purchased from Bio-Rad (California, USA). BCA protein content detection kit was purchased from KeyGEN Biotech Co. Ltd (Nanjing, China). Water used throughout all experiments was purified with the Millipore system.

SAS cells from an oral squamous cell carcinoma cell line were kindly donated by Prof. Fujii Masato (National Institute of Sensory Organs, National Tokyo Medical Center, Tokyo, Japan).³²

Preparation of CDs

Briefly, CS of 200 mg was dissolved in 10 mL water, and the solution was heated hydrothermally in a stainless steel autoclave at 200°C for 5 h. The obtained brown solution was cooled down to room temperature, and filtered through a 0.22 μm membrane to remove agglomerated particles. The purified CSCDs were lyophilized and stored at room temperature.

Characterization

Transmission electron microscopy (TEM) observation was performed using a FEI TecnaiG2 Spirit at an acceleration voltage of 120 kV. Fourier-transform infrared (FTIR) spectra were recorded by a Burker Vector 22 spectrometer. X-ray diffraction (XRD) measurement was carried out using a PANalytical X'Pert PRO diffractometer (Almelo, Netherlands) in conjunction with Cu $\text{K}\alpha$ radiation ($\lambda = 0.15418$ nm). X-ray photoelectron spectrometer (XPS, Thermo Scientific) were used to characterize the chemical composition using an Escalab 250 Xi X-ray photoelectron spectrometer. Absorption and fluorescence spectra were recorded at room temperature with a UV-2550 UV-vis spectrophotometer (Shimadzu, Japan) and Luminescence Spectrometer 55 (Perkin-Elmer), respectively. Fluorescence quantum yield was determined at 360 nm for excitation and 450 nm for emission in 0.10 M H_2SO_4 solution using quinine sulfate as the reference with a quantum yield of 54%. The effect of pH on the fluorescence (photoluminescence, PL) of CSCDs was examined in Britton–Robinson buffer solutions, which were prepared by 0.04 M each of H_3PO_4 , CH_3COOH and H_3BO_3 . Different pH values (from 2 to 11) were adjusted by 0.2 M NaOH. Moreover, CSCDs were incubated in Dulbecco's Modified Eagle Medium (DMEM) with 10% fetal bovine serum (FBS), FBS-free medium, phosphate buffer solution (PBS) and distilled water, respectively, in a fully humidified incubator at 37°C with 5% CO_2 to see the impact of these conditions.

Cell culture

SAS cells were seeded in a 24-well plate containing DME Medium with 10% FBS, and incubated in a fully humidified incubator at 37°C with 5% CO_2 . The cells cultured at approximately 70-80% confluence were used for further experiment.

Fluorescence labeling of SAS cells

CS and CSCDs were dissolved in DMEM medium with final concentrations (mg/mL) of 0.25, 0.5, 1, 2 and 4, and then filtered by the 0.2 μm Acrodisc syringe filter before being inoculated into cell dishes. Following attachment, SAS cells were incubated with 1 mL CS or CSCDs medium in $\Phi 20$ mm cell culture dishes at 37°C and 5% CO_2 for 4 h. The cells were washed with PBS buffer to remove unbound CS or CSCDs before imaging. Fluorescence imaging studies were performed with laser based point scanning FV 1000 confocal microscope (Olympus, Japan). Oil inserted 100 \times objective lens were used in the xy-mode with 800 \times 800 pixel resolution. Laser beams at 405 nm and 488 nm were used for excitation with emitted light collected between 425-475 nm and 500-600 nm, respectively. Native cells were also imaged under the same conditions as the control.

Cell viability analysis

Cell viability was detected using Cell Counting Kit-8 (CCK8) (Dojindo Laboratories, Kumamoto, Japan), according to the manufacturer's instructions. Briefly, CS and CSCDs were dissolved in DMEM, with the final concentrations (mg/mL) of 0.25, 0.5, 1, 2 and 4. SAS cells were seeded into a 96-well at bottom tissue culture plate with 8×10^3 cells for each well, incubated for 24 h and then treated with various concentrations of CS and CSCDs for 6 d. Cell viability was tested daily. SAS cells were incubated with DMEM containing 10% (v/v) CCK8 at 37°C for 1 h, and then supernatant was collected to test the absorbance. The absorbance at 450 nm with a reference wavelength of 630 nm was recorded by using a microplate reader (Well Scan MK3, Labsystems Dragon, Finland).

qRT-PCR analysis

SAS cells cultured with CS or CSCDs at various concentrations were incubated for 6 d at 37°C and then harvested by trypsin. The total RNA of cells was isolated using RNAiso Plus (TaKaRa, Shiga, Japan) according to the manufacturer's instructions. Reverse transcription (RT) was performed using a PrimeScript RT Reagent Kit (TaKaRa). Real-time quantitative reverse transcriptase-polymerase chain reaction (qRT-PCR) was performed with SYBR Premix Ex Taq (Takara). qRT-PCR amplification and fluorescence detection were performed using an Mx3000P Real-Time Cycler (Agilent Technologies, Santa Clara, CA, USA). The primers for the qRT-PCR are given in Table 1, which were designed by Takara Biotechnology Co., Ltd (Dalian, China). The results are comparative expression ratio to control for each sample using the CT method ($2^{-\Delta\Delta\text{CT}}$).

Table 1. Primer pairs used for the qRT-PCR studies

Gene	Sequence (5'→3')	Gene ID	Size (bp)
MMP2	CTCATCGCAGATGCCTGGAACAGCC TAGCCAGTCGGATTG	NM_004530	167
MMP9	TGGGCTACGTGACCTATGACATGCC CAGCCACCTCCACTCCTC	NM_004994.2	173
β -Actin	TGGCACCCAGCACAACTGAATAAG TCATAGTCCGCCTAGAAGCA	NM_0011101	187

Zymography

The proteolytic activity of MMPs was assessed by gelatin zymography as previously described.³³ SAS cells cultured with various concentrations of CS or CSCDs were incubated for 6 d and then rinsed with a serum-free medium. Condition medium was collected after incubating in the serum-free medium for 24 h and equal amounts of protein were used with each sample. Electrophoresis straps indicative of gelatinolytic activity were visualized by staining the gels with coomassie blue (0.5%, w/v), and gelatinolytic activities on the gel zymograph were visualized as clear bands against the blue background.

Statistical analysis

Statistical analysis for each sample was calculated using ANOVA. All data were reported as mean \pm standard deviation (SD). The significance was tested at $p < 0.05$.

Results and discussion

Optical and physicochemical properties of CS and CSCDs

CS was applied to synthesize CDs. The CS aqueous solution was transparent with light yellow even when supplemented at 20 mg/mL. It was found to be fluorescent under UV light as illustrated in Fig. 1(A). After heating hydrothermally for 5 h and filtering out the undissolved substance, a clear yellow solution of CSCDs was obtained, which exhibited bright fluorescence under UV light as illustrated in Fig. 1(B). The UV-vis absorption and PL spectra of CS and CSCDs excited at different wavelengths were thus investigated. It was observed that CS had a weak shoulder peak at 320 nm, the typical absorption of $n-\pi^*$ transition of C=O groups, while the absorption peak of CSCDs shifted to 315 nm, which was probably due to their dehydration and carbonization process during hydrothermal treatment. As the excitation wavelength increased from 300 nm to 440 nm with 20 nm increment, the emission of CS and CSCDs also shifted, reaching the peak intensity at 418 nm and 423 nm respectively, both under the excitation wavelength of 340

nm as illustrated in Fig. 1. This excitation wavelength dependent PL emission property was reported previously.³⁴⁻³⁶ It was believed that besides the quantum size effect^{37, 38} and surface defect,^{38, 39} the functional groups on the surface also contributed to PL. To investigate more properties of the CSCDs, a variety of characterizations were subsequently performed.

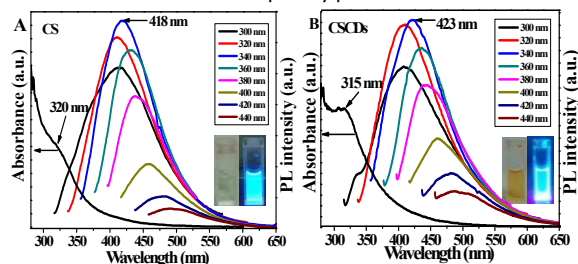


Fig. 1 UV-vis absorption and photoluminescent emission spectra of CS (A), and CSCDs (B) in aqueous solutions. Insets show the photographs of CS and CSCD solutions under the illumination of natural light (left) and UV light (312 nm, right).

The morphology and size of CSCDs were examined by TEM. As can be seen in Fig. 2, nanodots with an average diameter of 6 nm were developed, validating the formation of CSCDs. The size distribution obtained by measuring totally 80 CSCDs was in accordance with those reported previously.^{40, 41} Although the size exhibited a wide distribution, almost 65% of CSCDs was less than 10 nm.

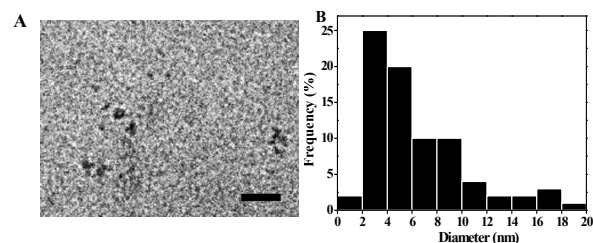


Fig. 2 Characterization of CSCDs. (A) Morphology observed with TEM (Scale bar: 20 nm), and (B) Size distribution of CSCDs.



To further investigate the impact of hydrothermal process on CS molecules, XRD characterization was applied. As shown in Fig. 3A, XRD of CSCDs show peaks at $2\theta = 23^\circ$ and 31° that are assigned to the diffraction of graphitic carbon, which are different from that of CS with one broad peak at $2\theta = 23^\circ$. This proves that CS decomposed to fractions (carbonization) during the hydrothermal process, which falls in line with TEM results.

Details of structural changes of CS were highlighted by the FTIR. As shown in Fig. 3B, the FTIR spectrum for CS showed the following functional groups: vibrations of the $-\text{OH}$ (3450 cm^{-1}), stretching vibrations of $\text{C}=\text{O}$ (around 1640 and 1410 cm^{-1}), $\text{S}=\text{O}$ (1250 cm^{-1}) and symmetric and asymmetric stretching vibrations of $\text{C}-\text{O}-\text{C}$ (around 1140 and 1075 cm^{-1}). After the hydrothermal process, N-H associations (3225 cm^{-1}), amido I $\text{C}=\text{O}$ bond (1680 cm^{-1}), amido II N-H bond (1620 cm^{-1}) and more $\text{C}-\text{O}-\text{C}$ bond (1140 cm^{-1}) were detected, indicating dehydration and decomposition of the CS into CSCDs. The CS and CSCDs both exhibit good hydrosolubility due to their abundant hydrophilic groups ($-\text{OH}$, $\text{C}=\text{O}$, and $\text{C}-\text{O}-\text{C}$).

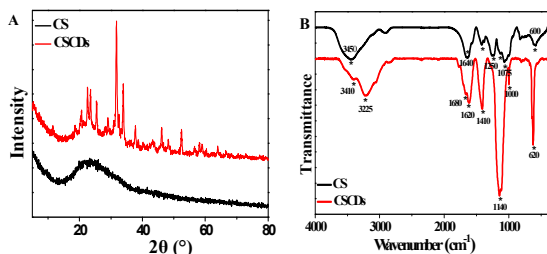


Fig. 3 Structural properties of CS and CSCDs. (A) XRD patterns; (B) FTIR characterization.

More structural insights could be obtained by XPS results. XPS spectra showed that CS (Fig. 4A) and CSCDs (Fig. 4B) were mainly composed of C (284.27 eV), O (532.04 eV) and N (398.80 eV). And their contents in CS were calculated to be 52.49% (C), 4.45% (N) and 43.06% (O), respectively, while 64.83% (C), 5.27% (N) and 29.91% (O) were detected in CSCDs, indicating the higher doping concentration of nitrogen in the CSCDs. The existence of nitrogen-rich functional groups, as excellent auxochromes, could be the reason for the significant enhancement in PL properties.⁴¹

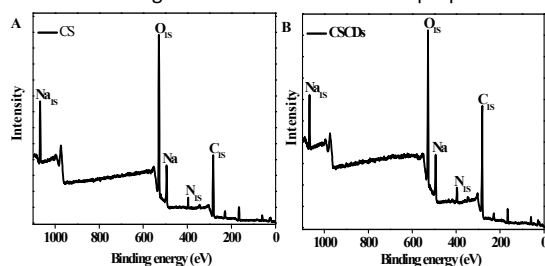


Fig. 4 XPS characterization of CS (A) and CSCDs (B).

CSCDs possessed pH-dependent luminescence slightly. As shown in Fig. 5A, their PL intensity varied within 25% when the pH changed from acidic to alkaline. The variation corresponded with the protonation and deprotonation of hydroxyl and carboxyl groups, which might cause electrostatic doping to CSCDs and shift the Fermi level. Under the physiological pH from 5 to 9, the PL intensity of CSCDs was relatively stable. Similar phenomenon was also observed when incubated in various culture conditions illustrated in Fig. 5B, although slight decrease in the PL intensity occurred in the FBS medium, indicating that agglomeration with proteins might occur during the incubation. In addition, CSCDs are photostable, which can be stored under light illumination conditions (data not shown). The quantum yield of CSCDs was 7.2%, higher than that of 6.7% with CS. These properties made CSCDs an ideal material for labeling biological samples.

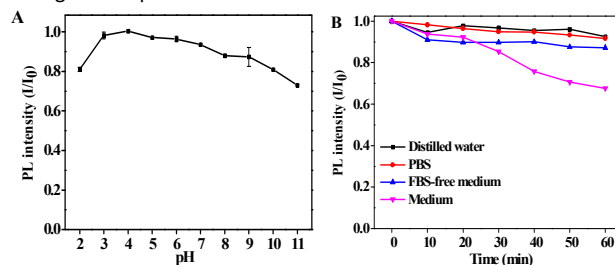


Fig. 5 Fluorescence responses of CSCDs to pH variation (A) and culture conditions without cell inoculation (B).

Cellular imaging of CSCDs

As illustrated in Fig. 6, after co-incubation with 1 mg/mL CSCDs for 4 h, the SAS cells showed blue and green fluorescence upon excitation at 405 nm and 488 nm , respectively. This multicolor imaging under different excitation wavelengths highlighted the fluorescent property of CSCDs. However, non-fluorescence was observed in the SAS cells co-incubated with 1 mg/mL CS or blank culture medium. Combining the confocal microscopy imaging with the knowledge that particles smaller than 100 nm can be enclosed within endocytic vesicles,⁴² we speculated that CSCDs enter the cells via endocytosis route, just like other CDs from different sources.^{43, 44} The fluorescent confocal images of the whole SAS cells incubated with CSCDs indicated that CSCDs could enter into the cells, while CS molecules were blocked from entering cells probably due to their long chains and complex configurations. The cell imaging also showed the dose dependent property, since cells co-incubated with 0.25 and 0.5 mg/mL CSCDs showed weaker fluorescence (data not shown), while CSCDs supplemented at 2 and 4 mg/mL exhibited cytotoxicity.

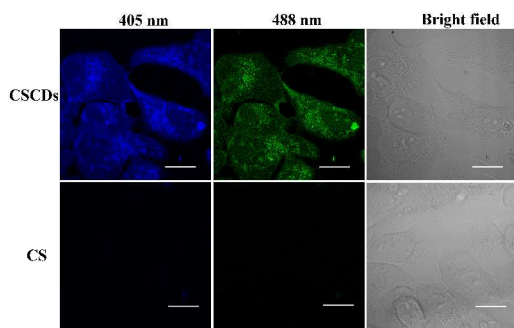


Fig. 6 Fluorescence image of SAS cells incubated with CSCDs and CS (Scale bar: 20 μm). The autofluorescence of cells was minimized by adjusting excitation intensity and PMT parameters.

Dose-dependent impact of CSCDs on the proliferation of SAS cells

For biomedical use, cytotoxicity is a key factor to be considered.⁴⁵ For this purpose, the viabilities of SAS cells incubated with CSCDs at 37°C were evaluated using the CCK8 assay with CS as the calibration. As shown in Fig. 7A, the dose-dependent in vitro cytotoxicity of CSCDs on the SAS cells was observed when CSCDs supplemented at 2 mg/L during 24 h. In contrast, CSCDs under 1 mg/L did not impose significant toxicity to SAS cells with long incubation time. As shown in Fig. 7B, more than 50% SAS cells were viable when treated with 0.5 mg/mL CSCDs for 6 d. Meanwhile, the result also indicated that CSCDs showed significant promotion effect for the SAS cells, which was time- and dose-dependent.

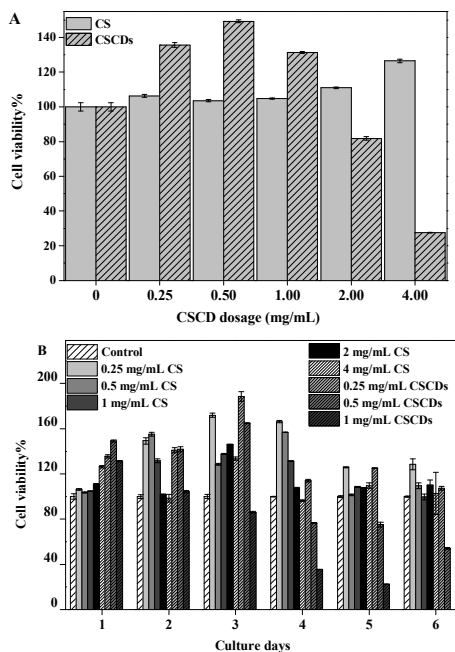


Fig. 7 Cell viability tested. (A) Dose-dependence, and (B) Proliferation of SAS cells.

CS as a component of ECM from which CSCDs were derived, has an effect on tumor cell proliferation. What is interesting is that CSCDs with 0.25 mg/mL also exhibited this effect. The result is similar to those previously reported due to the degradation of the ECM proteins which affected the biophysical microenvironment

associated with tumor cells,⁴⁶ and thus could be emerged as a particularly powerful regulator of the behavior of tumor cells.⁴⁷ As a result, CSCDs may be the fraction of CS promoted SAS proliferation, by nanoscale topography that closely mimics the product of the ECM degradation.

Invasion properties of SAS with CSCDs

CS polymer has been demonstrated to play an important role in creating microenvironment for protease activation by binding with MMPs.²⁵ Among the family members of MMPs, MMP2 and MMP9, which are also called gelatinases or type-IV collagenases, are closely connected with cancer progression,²⁸ mainly due to their role in degrading native type V, VII and X collagens, fibronectin, elastin and gelatin.⁴⁸

In order to determine the molecular mechanism underlying the effect of CSCDs on the potential metastasis of SAS cells, the expression of the genes encoding MMP2 and MMP9 in the SAS cell lines were analyzed by qRT-PCR. The results showed that CSCDs supplemented with 0.25 mg/mL up-regulated the gene expression, while CS exhibited the role at higher concentrations (Fig. 8A). Low molecular weight CS was reported to enhance CD44 cleavage and promote CD44-dependent cell migration in tumor cells,²⁴ which might be the case with the role of CSCDs in the cell invasion process.

Zymography analysis was performed to quantify the secretion of MMP2 and MMP9, which indicated their gelatinolytic activity in the cell culture supernatant collected on day 6 (Fig. 8B). The results indicated that neither the activity of MMP2 nor MMP9 showed an increase with CSCDs. It is worth noting that CS increased pro-MMP-9 amount with the concentrations of 0.5 and 1 mg/mL, but the active MMP9 had no change. This might be attributed to the change in CS structure during the preparation of CSCDs. The zymography results suggested that CSCDs and CS had no effect on the activities of MMP2 and MMP9 of the two-dimensional cultured SAS cells.

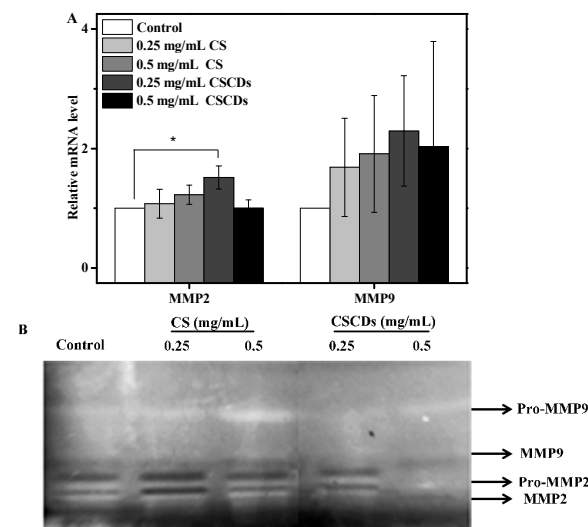


Fig. 8 Metastasis related gene and protein expression of SAS cells. (A) QRT-PCR analysis of the gene expression of MMP2 and MMP9

with β -actin as the internal control ($n=3, *P<0.05$). (B) Zymography analysis of the secretion of MMP2 and MMP9 by SAS cells.

In contrast to the high doses of CSCDs inducing cytotoxicity, these results showed that SAS cells responded to low doses of CSCDs by promoting cell proliferation (Fig. 7B) and improving gene expression for invasion (Fig. 8A), which might be explained as "hormesis",⁴⁹ a dose-response process: low concentration improves cell proliferation while high concentration exhibits toxic effect.^{50,51} This is particularly the case for investigating the toxicological effects of nanoparticles, which is markedly impacted by regulatory, and risk assessment considerations that are predicated on the assessment of high dose effects and the determination of toxic thresholds at fixed periods of observation.

CS not only promotes cell proliferation, but also improves the expression of invasion related genes,⁵² which have been broadly applied in simulating the component of ECM in the body.⁵³ Although CDs have been widely utilized owing to their unique physical and chemical properties,⁵⁴ there is no research so far to combine CS and CSCDs to investigate their influence on tumor cells. This study demonstrated that SAS cells cultured with CSCDs showed improved cell viability and expression of genes related to tumor invasion. CSCDs might affect the behaviors of the tumor cells through their nanoscale structures as previously reported.^{30, 55, 56} These results suggest that CSCDs closely mimic the extracellular matrix component on which tumor cells survive in vivo. Additionally, CS can stimulate the growth and differentiation of neurons and prevent normal brain synapses from disintegration after injury,⁵⁷ and CSCDs could be thus expected for this purpose for the future research while providing fluorescence labelling.

It also points out that the fluorescent CSCDs can be effective tool in investigating interactions of extracellular matrix with tumor cells, thus facilitating extracellular matrix based therapy in the cancer.

Conclusions

High solubility, good photostability, and low cytotoxicity make CSCDs suitable for biological imaging. Unlike most CDs prepared before, CSCDs prepared from CS retained CS properties to simulate ECM, and thus promoted the invasion and proliferation for SAS cells. On the other hand, compared to CS, CSCDs created nanoscale topography for SAS cells and enhanced the expression of their MMPs genes. As a result, CSCDs combined advantages of CDs and CS together, which was validated in our study for the first time, making them potential multifunctional materials for biomedical applications.

Acknowledgements

The authors would like to acknowledge the generous donation of SAS cells from Professor Fujii Masato at the National Institute of Sensory Organs, National Tokyo Medical Center, Tokyo, Japan. We thank Hao Wu for help with the TEM operation. Meanwhile, the assistance of Dr. Weiting Yu and Dr. Xiuli Wang with article writing is highly appreciated.

References

1. J. C. G. Esteves da Silva and H. M. R. Gonçalves, *Trac-Trend Anal. Chem.*, 2011, **30**, 1327-1336.
2. P.-C. Hsu, P.-C. Chen, C.-M. Ou, H.-Y. Chang and H.-T. Chang, *J. Mater. Chem. B*, 2013, **1**, 1774.
3. S. N. Baker and G. A. Baker, *Angew. Chem. Int. Ed. Engl.*, 2010, **49**, 6726-6744.
4. R. K. Shukla, J. Mirzaei, A. Sharma, D. Hofmann, T. Hegmann and W. Haase, *RSC Adv.*, 2015, **5**, 34491-34496.
5. K. Hola, A. B. Bourlinos, O. Kozak, K. Berka, K. M. Siskova, M. Havrdova, et al., *Carbon*, 2014, **70**, 279-286.
6. H. Li, Z. Kang, Y. Liu and S.-T. Lee, *J. Mater. Chem.*, 2012, **22**, 24230-24253.
7. B. Kong, A. Zhu, C. Ding, X. Zhao, B. Li and Y. Tian, *Adv. Mater.*, 2012, **24**, 5844-5848.
8. Y. Mao, Y. Bao, D. Han, F. Li and L. Niu, *Biosens. Bioelectron.*, 2012, **38**, 55-60.
9. G. Hong, S. Diao, A. L. Antaris and H. Dai, *Chem. Rev.*, 2015, DOI: 10.1021/acs.chemrev.5b00008.
10. S. Sahu, B. Behera, T. K. Maiti and S. Mohapatra, *Chem. Commun. (Camb)*, 2012, **48**, 8835-8837.
11. J. F. Y. Fong, S. F. Chin and S. M. Ng, *Sens. Actuators B Chem.*, 2015, **209**, 997-1004.
12. T. Kobayashi, H. Yan, Y. Kurahashi, Y. Ito, H. Maeda, T. Tada, et al., *Plos One*, 2013, **8**, 350-352.
13. A. P. T. Asimakopoulou, Achilleas D. Tzanakakis, George N. Karamanos, Nikos K., *In Vivo*, 2008, **22**, 385-389.
14. S. Yamada and K. Sugahara, *Curr. Drug Discov. Technol.*, 2008, **5**, 289-301.
15. C. M. Lee, T. Tanaka, T. Murai, M. Kondo, J. Kimura, W. Su, et al., *Cancer Res.*, 2002, **62**, 4282-4288.
16. N. G. Uhlman DL, *J. Pathol.*, 1999, **189**, 470-474.
17. A. L. M. Joji Iida, Jennifer R. Knutson, Leo T. Furcht and J. B. McCarthy, *Cancer Biol.*, 1996, **7**, 155-162.
18. Y. L. Yang, C. Sun, M. E. Wilhelm, L. J. Fox, J. Zhu and L. J. Kaufman, *Biomaterials*, 2011, **32**, 7932-7940.
19. S. Y. a. K. Sugahara, *Curr. Drug Discov. Technol.*, 2008, **5**, 289-301.
20. Y.-Q. L. Elizabeth M. Denholm, Paul J. Silver, *Eur. J. Pharmacol.*, 2001, **416**, 213-221.
21. D. Nikitovic, M. Assouti, M. Sifaki, P. Katonis, K. Krasagakis, N. K. Karamanos, et al., *Int. J. Biochem. Cell Biol.*, 2008, **40**, 72-83.
22. C. D. Nandini and K. Sugahara, *Adv. Pharmacol.*, 2006, **53**, 253-279.
23. E. Pantazaka and E. Papadimitriou, *Biochim. Biophys. Acta.*, 2014, **1840**, 2643-2650.
24. K. N. Sugahara, T. Hirata, T. Tanaka, S. Ogino, M. Takeda, H. Terasawa, et al., *Cancer Res.*, 2008, **68**, 7191-7199.
25. J. Iida, K. L. Wilhelmson, J. Ng, P. Lee, C. Morrison, E. Tam, et al., *Biochem. J.*, 2007, **403**, 553-563.
26. L. J. McCawley and L. M. Matrisian, *Curr. Opin. Cell Biol.*, 2001, **13**, 534-540.
27. S. Curran and G. I. Murray, *J Pathol*, 1999, **189**, 300-308.
28. M. Egeblad and Z. Werb, *Nat. Rev. Cancer*, 2002, **2**, 161-174.
29. J. Shi, A. R. Votrubka, O. C. Farokhzad and R. Langer, *Nano. letters*, 2010, **10**, 3223-3230.

30. M. Goldberg, R. Langer and X. Jia, *J. Biomater. Sci. Polym. Ed.*, 2007, **18**, 241-268.
31. K. Y. Tsang, M. C. Cheung, D. Chan and K. S. Cheah, *Cell Tissue Res.*, 2010, **339**, 93-110.
32. K. Okumura, A. Konishi, M. Tanaka, M. Kanazawa, K. Kogawa and Y. Niitsu, *J. Cancer Res. Clin. Oncol.*, 1996, **122**, 243-248.
33. P. M. Emma Pirila, Tuula Salo, Erkki Koivunen, Timo Sorsa, *Biochem. Biophys. Res. Commun.*, 2001, **287**, 766-774.
34. X. J. Mao, H. Z. Zheng, Y. J. Long, J. Du, J. Y. Hao, L. L. Wang, et al., *Spectrochim. Acta. A. Mol. Biomol. Spectrosc.*, 2010, **75**, 553-557.
35. D. Pan, J. Zhang, Z. Li, C. Wu, X. Yan and M. Wu, *Chem. Commun. (Camb)*, 2010, **46**, 3681-3683.
36. X. Yang, Y. Zhuo, S. Zhu, Y. Luo, Y. Feng and Y. Dou, *Biosens. Bioelectron.*, 2014, **60**, 292-298.
37. D. Chowdhury, N. Gogoi and G. Majumdar, *RSC Adv.*, 2012, **2**, 12156-12159.
38. X. Guo, C. F. Wang, Z. Y. Yu, L. Chen and S. Chen, *Chem. Commun. (Camb)*, 2012, **48**, 2692-2694.
39. A. Konwar, N. Gogoi, G. Majumdar and D. Chowdhury, *Carbohydr. Polym.*, 2015, **118**, 238-245.
40. V. Gupta, N. Chaudhary, R. Srivastava, G. D. Sharma, R. Bhardwaj and S. Chand, *J. Am. Chem. Soc.*, 2011, **133**, 9960-9963.
41. B. Shi, L. Zhang, C. Lan, J. Zhao, Y. Su and S. Zhao, *Talanta*, 2015, **142**, 131-139.
42. K.-I. Ogawara, M. Yoshida, K. Furumoto, Y. Takakura, M. Hashida, K. Higaki, et al., *J. Drug Target.*, 1999, **7**, 213-221.
43. M. Algarra, M. Perez-Martin, M. Cifuentes-Rueda, J. Jimenez-Jimenez, J. C. Esteves da Silva, T. J. Bandosz, et al., *Nanoscale*, 2014, **6**, 9071-9077.
44. B. Han, W. Wang, H. Wu, F. Fang, N. Wang, X. Zhang, et al., *Colloids Surf. B Biointerfaces*, 2012, **100**, 209-214.
45. H. U. Lee, S. Y. Park, E. S. Park, B. Son, S. C. Lee, J. W. Lee, et al., *Sci. Rep.*, 2014, **4**, 4665.
46. A. R. Anderson, A. M. Weaver, P. T. Cummings and V. Quaranta, *Cell*, 2006, **127**, 905-915.
47. A. Pathak and S. Kumar, *Integrative biology*, 2011, **3**, 267-278.
48. R. M. Senior, G. L. Griffin, C. J. Fliszar, S. D. Shapiro, G. I. Goldberg and H. G. Welgus, *J. Biol. Chem.*, 1991, **266**, 7870-7875.
49. I. Iavicoli, E. J. Calabrese and M. A. Nascarella, *Dose-response*, 2010, **8**, 501-517.
50. E. J. Calabrese and L. A. Baldwin, *Hum. Exp. Toxicol.*, 2002, **21**, 91-97.
51. M. A. Nascarella and E. J. Calabrese, *Dose-response*, 2012, **10**, 344-354.
52. P. Frankel, C. Pellet-Many, P. Lehtolainen, G. M. D'Abaco, M. L. Tickner, L. Cheng, et al., *Embo. Reports*, 2008, **9**, 983-989.
53. W. Schneiders, C. Rentsch, S. Rehberg, S. Rein, H. Zwipp and S. Rammelt, *Mater. Sci. Eng. C*, 2012, **32**, 1926-1930.
54. M. P. Sk, S. K. Sailapu and A. Chattopadhyay, *Chemphyschem.*, 2015, **16**, 723-727.
55. H. Mao, N. Kawazoe and G. Chen, *Colloids Surf. B Biointerfaces*, 2015, **126**, 63-69.
56. S. P. Pathi, D. D. W. Lin, J. R. Dorvee, L. A. Estroff and C. Fischbach, *Biomaterials*, 2011, **32**, 5112-5122.
57. S. E. Tully, R. Mabon, C. I. Gama, S. M. Tsai, X. Liu and L. C. Hsieh-Wilson, *J. Am. Chem. Soc.*, 2004, **126**, 7736-7737.